

Evolution of the barium abundance in the early Galaxy from a NLTE analysis of the Ba lines in a homogeneous sample of EMP stars[★]

S. M. Andrievsky^{1,2}, M. Spite¹, S. A. Korotin², F. Spite¹, P. François¹, P. Bonifacio^{1,3,★★}, R. Cayrel¹, and V. Hill¹

¹ GEPI, Observatoire de Paris, CNRS, Université Paris Diderot, 92125 Meudon Cedex, France
e-mail: monique.spite@obspm.fr

² Department of Astronomy and Astronomical Observatory, Odessa National University, Isaac Newton Institute of Chile, Odessa branch, Shevchenko Park, 65014 Odessa, Ukraine
e-mail: scan@deneb1.odessa.ua

³ Istituto Nazionale di Astrofisica, Osservatorio Astronomico di Trieste, via Tiepolo 11, 34143 Trieste, Italy

Received 1 September 2008 / Accepted 18 November 2008

ABSTRACT

Context. Barium is a key element in constraining the evolution of the (not well understood) r-process in the first galactic stars and currently the Ba abundances in these very metal-poor stars were mostly measured under the Local Thermodynamical Equilibrium (LTE) assumption, which may lead in general to an underestimation of Ba.

Aims. We present here determinations of the barium abundance taking into account the non-LTE (NLTE) effects in a sample of extremely metal-poor stars (EMP stars): 6 turnoff stars and 35 giants.

Methods. The NLTE profiles of the three unblended Ba II lines (4554 Å, 5853 Å, 6496 Å) have been computed. The computations were made with a modified version of the MULTI code, applied to an atomic model of the Ba atom with 31 levels of Ba I, 101 levels of Ba II, and compared to the observations.

Results. The ratios of the NLTE abundances of barium relative to Fe are slightly shifted towards the solar ratio. In the plot of [Ba/Fe] versus [Fe/H], the slope of the regression line is slightly reduced as is the scatter. In the interval $-3.3 < [\text{Fe}/\text{H}] < -2.6$, [Ba/Fe] decreases with a slope of about 1.4 and a scatter close to 0.44. For $[\text{Fe}/\text{H}] < -3.3$ the number of stars is not sufficient to decide whether [Ba/Fe] keeps decreasing (and then CD-38:245 should be considered as a peculiar “barium-rich star”) or if a plateau is reached as soon as $[\text{Ba}/\text{Fe}] \approx -1$. In both cases the scatter remains quite large, larger than what can be accounted for by the measurement and determination errors, suggesting the influence of a complex process of Ba production, and/or inefficient mixing in the early Galaxy.

Key words. stars: general – stars: abundances – Galaxy: halo – Galaxy: evolution – stars: supernovae: general – Galaxy: abundances

1. Introduction

In the framework of the ESO “large programme First stars”, very high quality spectra of extremely metal-poor (EMP) giants and turnoff stars were obtained with the high resolution spectrograph UVES fed with the VLT. In this sample, 33 giants and 18 turnoff stars are “normal metal-poor stars” (not carbon-rich). Among them 22 giants and 10 turnoff stars have $[\text{Fe}/\text{H}] \leq -3$. The main parameters of these stars can be found in Cayrel et al. (2004: “First stars V”) and Bonifacio et al. (2007: “First stars VII”, 2008: “First stars XII”). In François et al. (2007, “First stars VIII”) the abundance of the neutron capture elements has been studied in the sample of EMP giants. From an LTE analysis, it has been found that, generally speaking, the abundance ratios of these elements relative to iron ($[X/\text{Fe}]$) are very scattered, with sometimes a factor of more than one hundred between the abundance ratios of two stars with equal $[\text{Fe}/\text{H}]$. Moreover, on average, [Ba/Fe] increases from about -1.5 to $+0.2$ while $[\text{Fe}/\text{H}]$ increases from -3.6 to -2.6 . The important scatter of [Ba/Fe] (and $[\text{Sr}/\text{Fe}]$) vs. $[\text{Fe}/\text{H}]$ has been confirmed by Bonifacio et al. (2008, “First stars XII”) where the abundances in the sample of giants

are compared to the abundances in a sample of turnoff stars obtained in the same conditions. On the other hand, from a similar LTE analysis, e.g. Burris et al. (2000), Honda et al. (2004) or Lai et al. (2008) found abundance ratios that, in the same range of metallicity, show a similar behaviour. This general trend can also be traced from the rather low S/N measurements of Barklem et al. (2005) in a very large sample of 373 metal-poor stars, albeit with a larger scatter.

Generally, the barium abundance in metal-poor stars has been investigated under the LTE approximation. However, the NLTE corrections can be very significant, in particular at low metallicity (see Asplund 2005; Short & Hauschildt 2006) they could be at least partly responsible for the large scatter of the abundance ratios of the heavy elements at low metallicity. In order to determine reliable trends and scatters, and to properly trace the history of nucleosynthesis processes in the first stars, it is highly desirable to perform NLTE analyses.

There are several studies devoted to the determination of the NLTE barium abundance in metal-poor stars. Gigas (1988) performed NLTE modeling of the barium lines in the spectrum of the mildly metal deficient dwarf star Vega. Later, Mashonkina & Bikmaev (1996), and Mashonkina et al. (1999) estimated abundance correction for the cooler and more metal deficient dwarfs (down to $[\text{Fe}/\text{H}] = -2.5$). This work was continued by Mashonkina & Gehren (2000), Mashonkina et al. (2003) and

[★] Based on observations obtained with the ESO Very Large Telescope at Paranal Observatory (Large Programme “First Stars”, ID 165.N-0276; P.I.: R. Cayrel.

^{★★} CIFIST Marie Curie Excellence Team.

more recently by Mashonkina et al. (2008). In this last paper the authors study the abundance of the heavy elements in four very metal-poor stars with $[\text{Fe}/\text{H}] \approx -2.5$: one giant, HD 122 563, and three turnoff stars. Moreover Short & Hauschildt (2006), performed a theoretical analysis of the non-LTE effects on the Ba lines ($\lambda = 4554, 5853, 6141, 6496 \text{ \AA}$) for metallicities between $[\text{Fe}/\text{H}] = -1$ and -5 . They used NLTE models for these computations, but an interesting point is that they could show that the NLTE profiles based on NLTE models differ negligibly from the NLTE profiles computed from LTE models (as is generally done).

We present here the results of a direct application of an NLTE analysis to the sample of extremely metal-poor stars (turnoff stars and giants) previously analyzed in the “First stars” programme. In our previous papers (Andrievsky et al. 2007, 2008) we reported the sodium and aluminium NLTE abundances in these same stars.

This sample covers the region of metallicities from $[\text{Fe}/\text{H}] \approx -2.5$ to -4.0 . Such metal-poor stars have not been investigated up to now with the aim of deriving their NLTE barium abundances.

2. Observations and reduction

The sample of stars and the observational data are the same as discussed in previous papers: First Stars V, VII, VIII and XII (Cayrel et al. 2004; Bonifacio et al. 2007; François et al. 2007; and Bonifacio et al. 2008). In brief, the observations were performed with the VLT-UT2 and UVES (Dekker et al. 2000) with a resolving power $R \approx 45\,000$. The signal-to-noise ratio in the spectra of the giants is very high: ~ 130 per pixel (with an average of 5 pixels per resolution element) but it is lower for the turnoff stars (generally fainter), in particular in the $\lambda 4554 \text{ \AA}$ region where the strongest Ba line is located, at the very end of the spectra obtained with the “blue” camera.

The spectra were reduced using the UVES context (Ballester et al. 2000) within MIDAS.

Table 1 gives the NLTE barium abundances for our sample. They could be determined for only six (out of 18) turnoff stars, because even their strongest lines of Ba are very weak. The $\epsilon(\text{Ba})_{\text{LTE}}$ value, given in Col. 6 for comparison, has been borrowed from François et al. (2007) for the giants and Bonifacio et al. (2008) for the turnoff stars. In the last column is given the total number of Ba lines used for the computation. If $n = 3$, all the three lines $4554, 5853,$ and 6496 \AA have been computed, if $n = 2$ only 4554 and 6496 \AA could be used and if $n = 1$ only 4554 \AA . For the giants, an “m” indicates that the star has been found “mixed” in Spite et al. (2005). In this table, for the determination of the relative LTE and NLTE values we have adopted for the solar values $\log \epsilon(\text{Ba}) = 2.17$ (Asplund et al. 2005) at variance with François et al. 2007 who adopted $\log \epsilon(\text{Ba}) = 2.13$ (Grevesse & Sauval 2000).

3. NLTE calculations

The NLTE profiles of the barium lines were computed using a modified version of the MULTI code (Carlsson 1986). The modifications are described in Korotin et al. (1999).

For these computations we used Kurucz’s (1992) models (ATLAS9), after checking on some typical stars that the use of MARCS models (Gustafsson et al. 2008) as in Cayrel et al. (2004) would not introduce any significant difference.

As a rule, in the turnoff stars with $[\text{Fe}/\text{H}] < -2$, the barium abundance can be determined only from the resonance line at

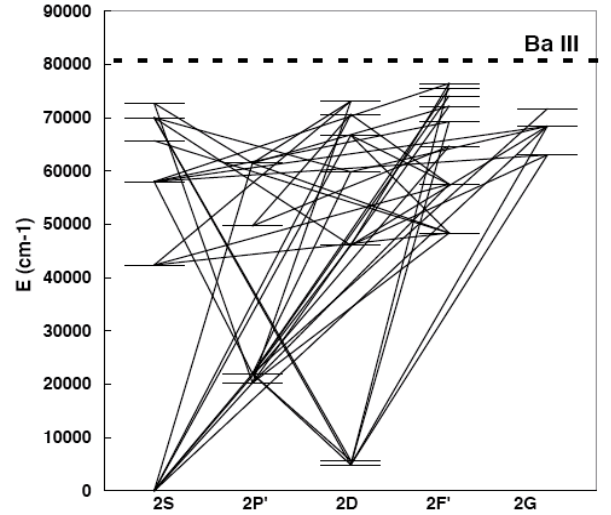


Fig. 1. The Grotrian diagramme for Ba II, only those transitions that were considered in detail, are indicated.

4554 \AA , but even this line becomes too weak at $[\text{Fe}/\text{H}] < -3.0$. In the giants, three lines can be traced down to $[\text{Fe}/\text{H}] \approx -3.0$, the resonance line and the two subordinate lines at 5853 and 6496 \AA ; at still lower metallicity only two lines (4554 and 6496 \AA) are still detectable.

3.1. Atomic model of Ba

Our barium model contains 31 levels of Ba I, 101 levels of Ba II with $n < 50$, and the ground level of Ba III ion. In the detailed consideration we included 91 bound-bound transitions between the first 28 levels of Ba II with $n < 12$ and $l < 5$. The other levels were used for the particle number conservation. The fine structure of the levels $5d^2D$ and $6p^2P^0$ was taken into account; the other levels were treated as single. The corresponding Grotrian diagram is shown in Fig. 1. Only those transitions that were considered in detail, are indicated. The energies of the levels are from Curry (2004). The oscillator strengths of the bound-bound transitions are from Wiese & Martin (1980), Warner (1968), and Miles & Wiese (1969). For the transitions between the seven low-lying levels we used the data from Davidson et al. (1992).

3.2. The different constants

A cause of uncertainty in the NLTE analysis of the barium spectrum is the scarce information about the photoionization cross-sections for the different levels. For the majority of the levels we used the results of the scaled Thomas-Fermi method application (Hofsaess 1979). For g-levels and levels with $n = 11$ we used the hydrogen-like approximation (Lang 1998, Eq. (1.230)).

Effective excitation electron collisional strengths for the transitions between the first levels ($6s^2S, 5d^2D$ and $6p^2P^0$) were used following Schoening & Butler (1998). Experimental cross-sections for the transitions $6s^2S - 7s^2S$ and $6s^2S - 6d^2D$ were taken from Crandall et al. (1974). Collisional rates for the transitions between sublevels $5d^2D, 6p^2P^0$ and $7s^2S, 6d^2D$, and between $7s^2S$ and $6d^2D$ were estimated with the help of the corresponding formula from Sobelman et al. (1981). For the rest of the allowed transitions, we used the van Regemorter (1962) formula, while for the forbidden transitions the Allen’s (1973) formula was used.

The rate of the collisional ionization from the ground level of Ba II was calculated using the corresponding formula in Sobelman et al. (1981). The use of experimental data of Peart et al. (1989) and Feeney et al. (1972) give the same results. For the other levels, Drawin’s (1961) formula was used.

Inelastic collisions of barium atoms with hydrogen atoms may play a significant role in the cool star atmospheres. They have been taken into account through the formula of Steenbock & Holweger (1984). A correcting factor of 0.1 was derived as a result of the experimental fitting of the barium lines in solar spectrum. Collisions with atomic hydrogen for the forbidden transitions were not taken into account, but we checked that the resulting uncertainty about the equivalent width of the lines, computed by the method of Takeda (1991), does not exceed 0.5%.

The odd barium isotopes have hyper-fine splitting of their levels and thus several HFS components for each line. As was demonstrated by Mashonkina et al. (1999), a three-component structure is sufficient to describe the 4554 Å barium line (see also Rutten 1978). This line was fitted in the solar spectrum by adopting the even-to-odd abundance ratio of 82:18 (Cameron 1982). Since metal deficient stars are supposed to include a larger fraction of the material synthesized in SNe II through the pure r-process, we used an even-to-odd ratio 50:50 for the stars. Nevertheless, we checked that the resulting difference in the equivalent widths of the 4554 Å line due to this change in the even-to-odd ratio is very small. (As a consequence, from our spectra it is not possible to estimate the abundance ratios of the different isotopes of Ba from our spectra, higher resolution would be necessary.)

Radiative damping constants are from Mashonkina & Bikmaev (1996), Stark broadening parameters are from the VALDatabase (<http://ams.astro.univie.ac.at/~vald>). Since the classical van der Waals formula underestimates the effect of the interaction with neutral particles, the broadening parameters were found by comparing the observed lines in the solar spectrum (Kurucz et al. 1984) with a synthetic spectrum computed with the solar model of Kurucz (1996). The best agreement was obtained for $\log\epsilon(\text{Ba}) = 2.17$ (Fig. 2), in good agreement with the estimation of the solar abundance of barium of Asplund et al. (2005).

The oscillator strengths of the lines components and the corresponding HFS shifts, as well as the broadening parameters are given in Table 2. For the Van der Waals constant C_6 we have adopted the definition of Unsöld (1968, Eqs. (82), (47)): $C_6 = \Delta\omega r^6/2\pi$.

3.3. Non-LTE effects

The profiles of the barium lines are rather sensitive to the NLTE effects, in particular in metal-poor stars with rather high temperature. The NLTE correction sign changes when the temperature and the metallicity change. Mashonkina et al. (1999) discuss in detail this behaviour in detail for turnoff metal-poor stars. Since the abundance of barium at a given metallicity is very scattered, it is important to note that the NLTE corrections are very sensitive not only to the metallicity of the model but also to the barium abundance itself (the equivalent width of the line).

- The resonance line or the low excitation subordinate lines that are used for the determination of the barium abundance can show substantial nonequilibrium excitation effects. In a metal-poor atmosphere, since there are few electrons and thus few collisions, the radiative processes cause the departure from equilibrium in the atomic level populations even in the deep

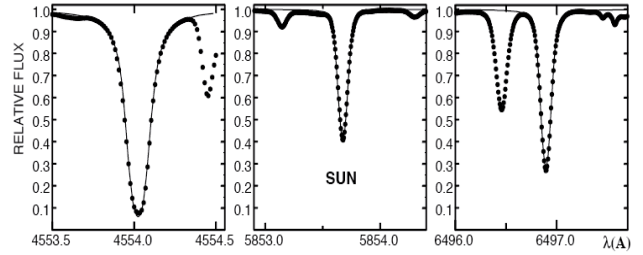


Fig. 2. Profile fitting for the barium lines in the solar spectrum with $\log\epsilon(\text{Ba}) = 2.17$.

atmospheric layers. If the mean intensity of the radiative field in the line frequencies J_ν exceeds the Planck intensity B_ν , then an enhanced photoexcitation depopulates the lower atomic levels and overpopulates the upper ones (this “pumping” is described e.g. in Bruls et al. 1992, or Asplund 2005). The depth of the effective formation of the radiation in b-b transitions changes significantly with the metallicity (and the corresponding barium abundance) of the star (Fig. 3). This explains the dependence of the NLTE correction on $[\text{Fe}/\text{H}]$ (Figs. 4 and 5). The lower the metallicity of the model, the deeper in the atmosphere is the line formation level (Fig. 3).

- Another mechanism causing the deviations from LTE is the so called UV overionization from the 6p level. In the atmosphere of turnoff or RGB stars, Ba II is the dominant species and generally this implies that overionization does not significantly affect the line formation. But for extremely metal-poor stars, already at $\tau_{5000} = 1$ the mean intensity exceeds the Planck intensity at the frequency of the ionization threshold of the 6p level. As a result this level is significantly depopulated.

These effects are very sensitive to the metallicity of the model, the physical conditions and the characteristics of the radiation in the layers where the barium lines are formed. In Fig. 3 the ratio of the source function to the Planck function is plotted for two giant stars with the same parameters $T_{\text{eff}} = 5250 \text{ K}$, $\log g = 1.5$, $V_t = 2 \text{ km s}^{-1}$, $[\text{Ba}/\text{Fe}] = -0.5$, but with different metallicities: $[\text{Fe}/\text{H}] = -2.0$ and -3.0 . The formation depth of the three lines used for the determination of the Ba abundance ($\lambda = 4554, 5853, 6496 \text{ Å}$) is indicated in the figure. It can be seen that S_I/B_ν is larger than 1 at the depth of the line formation for the three considered lines for $[\text{Fe}/\text{H}] = -3.0$. In this case, NLTE effects make the line weaker. The model with a higher metal abundance produces another picture. While two lines 5853 Å and 6496 Å are formed in that region where $S_I/B_\nu > 1$, the resonance line is formed significantly higher in atmosphere, and for this line $S_I/B_\nu < 1$. This line is made stronger as a result of the departure from LTE.

As an illustration we show in Figs. 4 (giants), and 5 (turnoff stars) how the NLTE correction depends on the metallicity for different effective temperatures. For the giant stars we used $[\text{Ba}/\text{Fe}] = -0.5$, while for dwarfs $[\text{Ba}/\text{Fe}] = 0.0$. These values are typical of the observations. (In turnoff stars if $[\text{Fe}/\text{H}] = -3.0$ and $[\text{Ba}/\text{Fe}] = -0.5$, the strongest barium line is very weak ($W < 4 \text{ mÅ}$) and since it is located at the end of the spectra it is generally not detectable). In fact the main parameter which determines the NLTE correction is $[\text{Ba}/\text{H}]$, as can be seen in Fig. 4. Our corrections for the 4554 Å line are in good agreement with those of Mashonkina & Bikmaev (1996) computed for dwarfs and $[\text{Fe}/\text{H}] = -2$.

In giant stars (Fig. 4), the NLTE correction for the two lines at 4554 and 5853 Å can be positive or negative depending

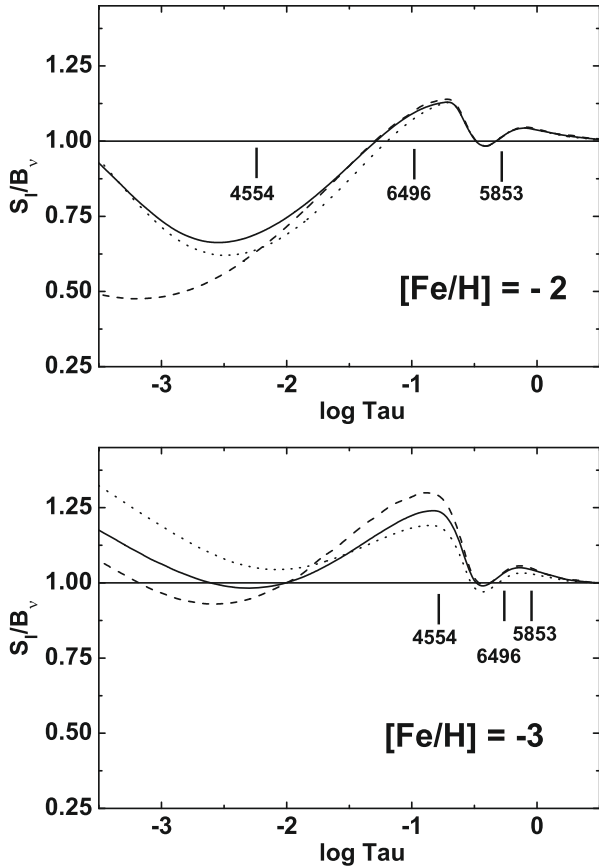


Fig. 3. Ratio S_l/B_v (Source function over Planck function) vs. the optical depth for the models $T_{\text{eff}} = 5250$ K, $\log g = 1.5$, $[\text{Fe}/\text{H}] = -2.0$ and -3.0 . The dashed line represents the 4554 Å line, the solid line the 5853 Å line and the dotted line the 6496 Å line.

on the effective temperature. A similar conclusion was obtained by Short & Hauschildt (2006). For the line 4554 Å we found that LTE and NLTE profiles coincide at $[\text{Fe}/\text{H}] = -2.5$, while Short & Hauschildt (2006) found such a coincidence at $[\text{Fe}/\text{H}] = -3.0$. Our computations (NLTE line transfer with an LTE background model) cannot be directly compared to those of Short & Hauschildt who used NLTE line transfer on an NLTE background model. In spite of this, the predictions of the two are qualitatively similar, with moderate quantitative disagreement. Part of the disagreement may, indeed, be due to the difference in the adopted background models, but part of it may also be due to the differences in the model atoms employed in the two computations. Some examples of the calculated profiles are given in Fig. 6.

3.4. Line profile fitting

It should be stressed that the NLTE corrections given in Figs. 4 or 5 should not be used to determine a precise value of the NLTE abundance of barium in metal-poor stars, since this correction depends critically on several parameters ($[\text{Ba}/\text{H}]$, v_t). The best way to determine the Ba abundance is to calculate the NLTE profiles directly, and to compare them to the observed profiles. Such an approach was used in this paper. The profile fitting for some stars is displayed in Fig. 7.

The mean NLTE barium abundances of the stars are listed in Table 1. The small difference between the $[\text{Ba}/\text{Fe}]$ ratio found

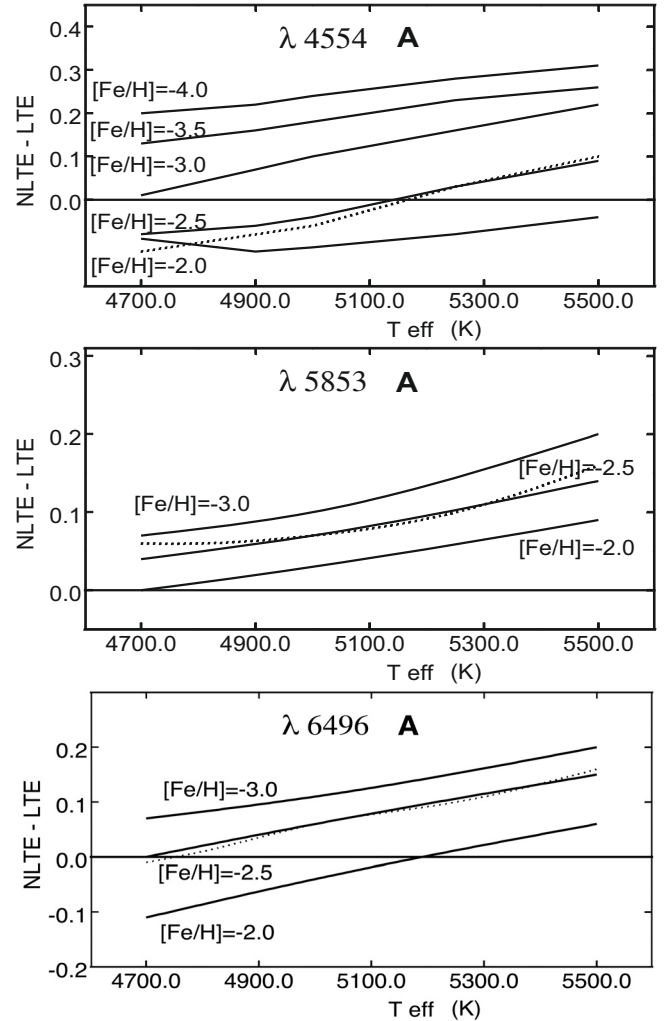


Fig. 4. NLTE corrections computed as a function of the temperature of the model, for several metallicities. The calculations are performed for $\log g = 1.5$ and $[\text{Ba}/\text{Fe}] = -0.5$ (solid lines). However, the computations have been done also for $[\text{Fe}/\text{H}] = -3.0$ and $[\text{Ba}/\text{Fe}] = 0.0$, thus $[\text{Ba}/\text{H}] = -3.0$ (dotted lines). It can be seen that the correction is then very similar to the correction computed for $[\text{Fe}/\text{H}] = -2.5$ and $[\text{Ba}/\text{Fe}] = -0.5$ (thus also with $[\text{Ba}/\text{H}] = -3.0$). The main parameter that determines the NLTE correction, is indeed $[\text{Ba}/\text{H}]$ and *not* $[\text{Fe}/\text{H}]$.

for HD 122563 in Mashonkina et al. (2008) and in our paper, can be explained by the different values adopted for the gravity. When several Ba lines are detected in the spectra of a star, the abundances deduced from the different lines agree within ± 0.1 dex. This value can be considered as the observational error. The total error is the quadratic sum of this error and of the error due to the stellar parameter uncertainties. The largest uncertainty arises from the uncertainties in the temperature and the gravity of the stars. We estimate that the total error on $[\text{Ba}/\text{Fe}]$ is close to 0.2 dex.

4. Discussion

4.1. Global trend

The behavior of the ratio $[\text{Ba}/\text{Fe}]$ vs. metallicity for the investigated stars is displayed in Fig. 8.

The turnoff and the giant stars show a similar behaviour (as judged from the few dwarfs for which Ba was measurable). There is no difference in the behaviour of mixed giants (stars

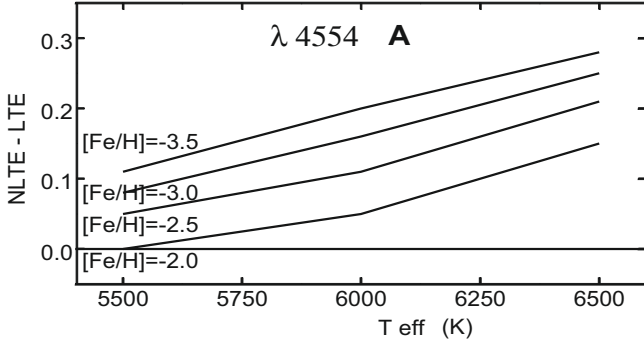


Fig. 5. NLTE corrections computed as a function of the temperature of the dwarf models, for several metallicities. All calculations are performed with $[\text{Ba}/\text{Fe}] = 0.0$ and $\log g = 4.5$.

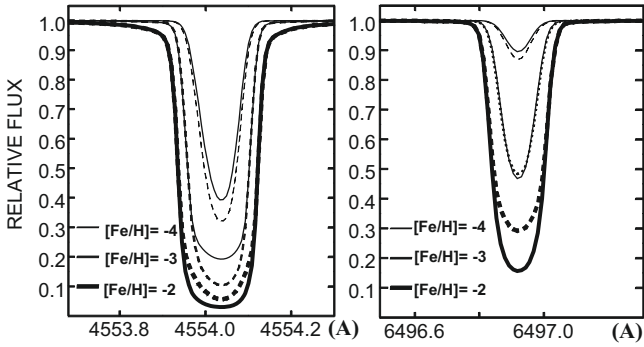


Fig. 6. LTE (dashed lines) and NLTE (solid lines) profiles calculated for $T_{\text{eff}} = 4800$ K, $[\text{Ba}/\text{Fe}] = 0.0$ and $\log g = 1.5$.

located above the Luminosity Function Bump: Spite et al. (2005, 2006) and the low RGB giants. Barium is not affected by mixing along the RGB.

In François et al. (2007) it has been shown from an LTE analysis that in the interval $-3.5 < [\text{Fe}/\text{H}] < -2.6$, the abundance of barium decreases rapidly with the metallicity, in agreement with previous works in the literature. Our NLTE analysis of the barium lines in the same extremely metal-poor star spectra has led to some *slight* shifts of the derived individual LTE $[\text{Ba}/\text{Fe}]$ ratios toward the solar ratio, but the main tendency is only slightly changed.

Globally the results may be summarised as follows (see Fig. 8):

Below the metallicity $[\text{Fe}/\text{H}] \approx -3.0$, the mean value of $[\text{Ba}/\text{Fe}]$ is negative as found in François et al. (2007).

The slope of the NLTE value of $[\text{Ba}/\text{Fe}]$ vs. $[\text{Fe}/\text{H}]$ is a little shallower than in LTE: the slope of the regression computed in the interval $-3.6 < [\text{Fe}/\text{H}] < -2.6$ is about 1.14 ± 0.12 in NLTE rather than 1.40 ± 0.18 under LTE assumption (Fig. 8). This small variation of the slope was expected by Mashonkina et al. (2008). The slope is compatible with a secondary production of Ba.

In the region $-3.6 < [\text{Fe}/\text{H}] < -2.6$, the scatter around the regression line of the $[\text{Ba}/\text{Fe}]$ vs. $[\text{Fe}/\text{H}]$ plot (Fig. 8) is a little smaller (0.44) for the NLTE values than for the LTE values (0.52), but it remains very large, much larger than observed for the abundances of other elements (where it is generally smaller than 0.2 dex). This scatter strongly exceeds what is expected from the measurement and determination errors, and illustrates the decoupling between iron and Ba nucleosyntheses. This point remains valid when using Mg (rather than Fe) as a reference element, suggesting also a decoupling between the production of Mg (hydrostatic burning) and Ba (r-process).

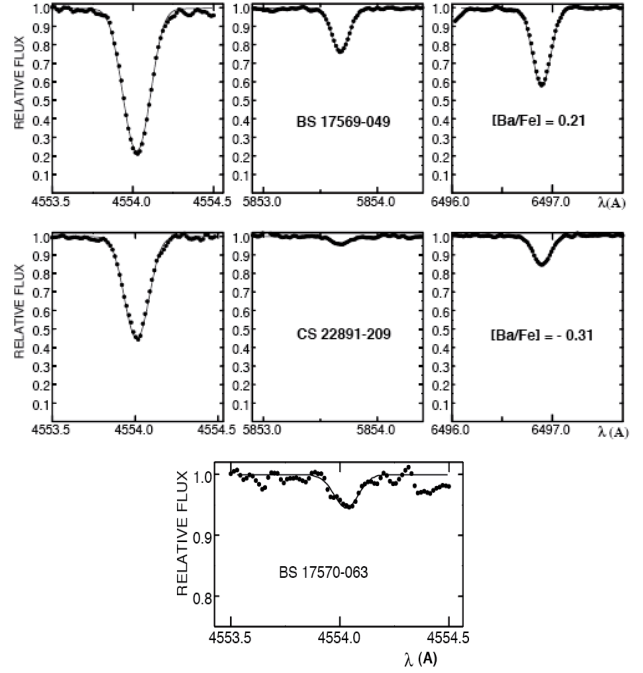


Fig. 7. Profile fitting for the barium lines in two giant stars (BS 17569-049 and CS 22891-209) and a turnoff star (BS 17570-063). In this last case only the 4554 Å line is visible.

In the extremely low metallicity domain ($[\text{Fe}/\text{H}] < -3.5$), the mean behaviour of $[\text{Ba}/\text{Fe}]$ is not clear. At this very low metallicity, the barium abundance could be estimated in only three “normal” stars. (CD -38:245, CS 22172-002 and CS 22885-096). In these stars $[\text{Ba}/\text{Fe}]$ is around -0.7 suggesting that a “plateau” of $[\text{Ba}/\text{Fe}]$ is reached. But for two other stars, only limits could be measured and for one of them it is rather low: $[\text{Ba}/\text{Fe}] < -1.37$.

4.2. A complex trend?

At very low metallicity ($[\text{Fe}/\text{H}] < -2.5$), the behaviour of $[\text{Ba}/\text{Fe}]$ with $[\text{Fe}/\text{H}]$ (Fig. 8) can be interpreted in three different ways:

1. Our Fig. 8 can be interpreted, as proposed by François et al. (2007), by a very large scatter of $[\text{Ba}/\text{Fe}]$ in the region $-3.2 < [\text{Fe}/\text{H}] < -2.8$: a factor of about 1000 from star to star, and (for $[\text{Fe}/\text{H}] < -3.3$) a plateau close to the value $[\text{Ba}/\text{Fe}] = -1$. This interpretation was suggested by François et al. (2007) after merging their measurements with those of Honda et al. (2004). But it seems that there is a systematic difference between these two sets of measurements: in Fig. 10 of François et al. the data points from Honda et al. seem to be systematically offsetted in $[\text{Fe}/\text{H}]$ and $[\text{Ba}/\text{Fe}]$ compared to the points of François et al. (2007). The difference is mainly due to the adoption of a lower microturbulent velocity by Honda et al. (2004). This systematic shift could be responsible, at least partly, for the very large scatter without any defined trend, suggested by François et al. (2007) in the region $-3.2 < [\text{Fe}/\text{H}] < -2.8$.
2. When only our measurements are taken into account (Fig. 8), and as a consequence, all the stars in the graph are studied in

Table 1. Adopted model and NLTE barium abundance for our sample of stars.

Star	T_{eff} , (K)	$\log g$	v_t , (km s $^{-1}$)	[Fe/H]	$\epsilon(\text{Ba})_{\text{LTE}}$	$\epsilon(\text{Ba})_{\text{NLTE}}$	[Ba/H] $_{\text{NLTE}}$	[Ba/Fe] $_{\text{NLTE}}$	Rem	
Turnoff stars										
BS 17570-063	6240	4.8	0.5	-2.92	-1.05	-0.83	-3.00	-0.08	1	
CS 22948-093	6360	4.3	1.2	-3.30	-0.90	-0.83	-3.00	+0.30	1	
CS 22966-011	6200	4.8	1.1	-3.10	-0.95	-0.73	-2.90	+0.20	1	
CS 29506-007	6270	4.0	1.7	-2.91	-0.55	-0.23	-2.40	+0.51	1	
CS 29506-090	6300	4.3	1.4	-2.83	-1.00	-0.63	-2.80	+0.03	1	
CS 30301-024	6330	4.0	1.6	-2.75	-0.85	-0.53	-2.70	+0.05	1	
Giants										
1	HD 2796	4950	1.5	2.1	-2.47	-0.48	-0.46	-2.63	-0.12	3, m
2	HD 122 563	4600	1.1	2.0	-2.82	-1.59	-1.45	-3.62	-0.80	3, m
3	HD 186 478	4700	1.3	2.0	-2.59	-0.50	-0.45	-2.62	-0.03	3, m
4	BD +17:3248	5250	1.4	1.5	-2.07	+0.75	+0.48	-1.69	+0.38	3, m
5	BD -18:5550	4750	1.4	1.8	-3.06	-1.67	-1.45	-3.62	-0.56	3
6	CD -38:245	4800	1.5	2.2	-4.19	-2.82	-2.50	-4.67	-0.48	1, m
7	BS 16467-062	5200	2.5	1.6	-3.77	<-2.76	<-2.35	<-4.52	<-0.75	
8	BS 16477-003	4900	1.7	1.8	-3.36	-1.68	-1.40	-3.57	-0.21	2
9	BS 17569-049	4700	1.2	1.9	-2.88	-0.55	-0.50	-2.67	+0.21	3, m
10	CS 22169-035	4700	1.2	2.2	-3.04	-2.10	-1.95	-4.12	-1.08	2, m
11	CS 22172-002	4800	1.3	2.2	-3.86	-2.90	-2.60	-4.77	-0.91	1,
12	CS 22186-025	4900	1.5	2.0	-3.00	-0.85	-0.72	-2.89	+0.11	3, m
13	CS 22189-009	4900	1.7	1.9	-3.49	-2.65	-2.40	-4.57	-1.08	1,
14	CS 22873-055	4550	0.7	2.2	-2.99	-1.31	-1.15	-3.32	-0.33	3, m
15	CS 22873-166	4550	0.9	2.1	-2.97	-1.54	-1.32	-3.49	-0.52	3, m
16	CS 22878-101	4800	1.3	2.0	-3.25	-1.70	-1.35	-3.52	-0.27	2, m
17	CS 22885-096	5050	2.6	1.8	-3.78	-2.75	-2.50	-4.67	-0.89	1
18	CS 22891-209	4700	1.0	2.1	-3.29	-1.71	-1.43	-3.60	-0.31	3, m
19	CS 22892-052*	4850	1.6	1.9	-3.03	+0.11	-0.03	-2.20	+0.83	3
20	CS 22896-154	5250	2.7	1.2	-2.69	-0.05	-0.13	-2.30	+0.39	3
21	CS 22897-008	4900	1.7	2.0	-3.41	-2.28	-2.15	-4.32	-0.91	1
22	CS 22948-066	5100	1.8	2.0	-3.14	-1.95	-1.75	-3.92	-0.78	1, m
23	CS 22949-037*	4900	1.5	1.8	-3.97	-2.42	-2.25	-4.42	-0.45	1, m
24	CS 22952-015	4800	1.3	2.1	-3.43	-2.63	-2.35	-4.52	-1.09	1, m
25	CS 22953-003	5100	2.3	1.7	-2.84	-0.22	-0.23	-2.40	+0.44	3
26	CS 22956-050	4900	1.7	1.8	-3.33	-1.98	-1.73	-3.90	-0.57	1
27	CS 22966-057	5300	2.2	1.4	-2.62	-0.73	-0.73	-2.90	-0.28	2
28	CS 22968-014	4850	1.7	1.9	-3.56	<-3.20	<-2.80	<-4.97	<-1.41	
29	CS 29491-053	4700	1.3	2.0	-3.04	-1.80	-1.52	-3.69	-0.65	3, m
30	CS 29495-041	4800	1.5	1.8	-2.82	-1.34	-1.06	-3.23	-0.41	3
31	CS 29502-042	5100	2.5	1.5	-3.19	-2.75	-2.40	-4.57	-1.38	1
32	CS 29516-024	4650	1.2	1.7	-3.06	-1.83	-1.45	-3.62	-0.56	3
33	CS 29518-051	5200	2.6	1.4	-2.69	-1.01	-0.60	-2.77	-0.08	3, m
34	CS 30325-094	4950	2.0	1.5	-3.30	<-3.05	<-2.85	<-5.02	<-1.72	
35	CS 31082-001	4825	1.5	1.8	-2.91	+0.39	+0.05	-2.12	+0.79	3

An asterisk after the name of the star means that the star is carbon-rich. In the last column is given the number of Ba lines used for the computation; the letter m indicates that the giant has been found “mixed” (see text).

a very homogeneous way, it becomes clear that in the interval $-3.6 < [\text{Fe}/\text{H}] < 2.5$, $[\text{Ba}/\text{Fe}]$ increases with $[\text{Fe}/\text{H}]$ with a slope close to ≈ 1.14 (when the non-LTE effects are taken into account).

A problem is to know what happens at lower metallicity. For $[\text{Fe}/\text{H}] < -3.6$ the decrease of $[\text{Ba}/\text{Fe}]$ could continue and then 5 stars would seem Ba-rich with the definition $[\text{Ba}/\text{Fe}] > [\text{Ba}/\text{Fe}] + 2\sigma$:

- the two carbon rich stars (CS 22892-052 (Snedden et al. 1996, and CS 22949-037 Depagne et al. 2002);
- the well known r-rich star CS 31082-001 (see Cayrel et al. 2001; Hill et al. 2002);
- CD-38:245, the most metal-poor star of the sample. In this star François et al. measured an upper limit of the europium abundance: $[\text{Eu}/\text{Fe}] < +0.38$. According to the definition (Barklem et al. 2005; Beers & Christlieb 2005) of the r-I class of “moderately r-rich stars”

($+0.3 < [\text{Eu}/\text{Fe}] < +1.0$) the upper limit of the Eu abundance may bring CD-38:245 in this class;

- a turnoff star, CS 22948-093. In this kind of star it would be impossible to measure the europium abundance even if it is r-rich with $[\text{Eu}/\text{Fe}] = 1$.

All these stars are or could be peculiar (two of them are well known very r-rich stars).

However if we suppose that in “normal” stars $[\text{Ba}/\text{Fe}]$ decreases continuously in the interval $-4.2 < [\text{Fe}/\text{H}] < -2.5$ with a uniform scatter ($\sigma = 0.44$), then 4 stars (over 38) are outside the two sigma limits (3 on one side and 1 on the other side). This is more than what it is expected for a Gaussian population (only 5%).

3. A third interpretation would combine a decrease of $[\text{Ba}/\text{Fe}]$ only in the range $-3.3 < [\text{Fe}/\text{H}] < -2.5$ and then a plateau which would determine the mean value of the ratio $[\text{Ba}/\text{Fe}]$ in the early Galaxy: $[\text{Ba}/\text{Fe}] \approx -0.7$ from this

Table 2. Parameters of the barium lines. $C_6 = \Delta\omega r^6/2\pi$, following (Unsöld 1968), in $\text{cm}^6 \text{s}^{-1}$.

$\lambda(\text{\AA})$	E_i	E_k	HFS $\Delta\lambda$	f	f	γ_{rad}	$\log C_6$
	eV	eV	mÅ	solar	50:50	s^{-1}	
4554.03	0.00	2.72	0	0.597	0.364	1.58×10^8	-31.3
			18	0.081	0.227		
			-34	0.049	0.137		
5853.70	0.60	2.72	-	0.025	-	1.58×10^8	-30.4
6496.90	0.60	2.51	0	0.086	-	1.25×10^8	-31.1
			-4	0.012	-		
			9	0.007	-		

NLTE analysis. The value of this plateau would define the yields of barium (relative to iron) in the massive primitive supernovae. If we consider only the stars with $[\text{Fe}/\text{H}] < -3.7$, the scatter around $[\text{Ba}/\text{Fe}] = -0.7$ is rather small, but there are 2 stars with upper limits that increase this scatter. If a plateau exists, it could suggest a production of Ba independent of the metallicity in the primitive supernovae.

The analysis of a larger sample of EMP stars with $[\text{Fe}/\text{H}] < -3.3$ would obviously help in the interpretation of the results.

5. Conclusion

We present here a homogeneous determination of the abundance of Ba in a sample of extremely metal-poor stars (turnoff and giant stars) taking into account the non-LTE effects.

There is a good agreement between the abundances of turn off stars, unmixed giants (low RGB) and “mixed” giants (stars located in the HR diagram higher than the Luminosity function bump). In the giant stars the abundance of barium does not depend on the deep mixing inside the star.

The NLTE abundances are free from the approximations made in the LTE determinations. The trend of $[\text{Ba}/\text{Fe}]$ versus $[\text{Fe}/\text{H}]$ is refined: less scatter, and a better defined and shallower slope. The slope is compatible with a secondary process. The general behaviour would be the same if Mg (rather than Fe) was the reference element.

The scatter of $[\text{Ba}/\text{Fe}]$, although reduced, is large, and cannot be explained by the determination errors: it suggests the influence of several factors. The contribution of one (or more) additional “r” process has been invoked in the literature (see François et al. and references therein 2007; Travaglio et al. 2004; Wasserburg & Qian 2008). Also, an extremely efficient galactic mixing is excluded.

The behaviour of $[\text{Ba}/\text{Fe}]$ with $[\text{Fe}/\text{H}]$ (Fig. 8) could be described in two different ways. For a decreasing metallicity:

1. the mean value of $[\text{Ba}/\text{Fe}]$ decreases linearly with a large (uniform) scatter and a few outliers;
2. the mean value of $[\text{Ba}/\text{Fe}]$ decreases linearly in the interval $-2.5 > [\text{Fe}/\text{H}] > -3.6$, and then reaches a plateau.

The number of observed stars at very low metallicity is obviously too low to reach any firm conclusion about a possible plateau, that could suggest a production of barium at low metallicity independent of the metallicity. Surveys detecting extremely metal-poor stars, and the spectroscopic observations of the detected stars, are required.

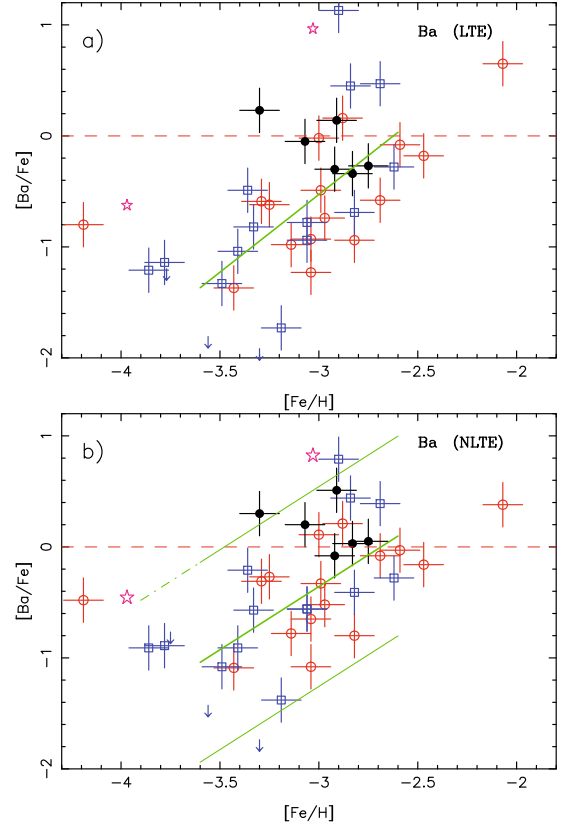


Fig. 8. $[\text{Ba}/\text{Fe}]$ vs. $[\text{Fe}/\text{H}]$ in our sample of stars computed with the LTE hypothesis (plot **a**) and taking into account the NLTE effects (plot **b**). The values of $[\text{Ba}/\text{Fe}]$ have been computed with $\log\epsilon(\text{Ba}) = 2.17$ (Asplund et al. 2005) at variance with François et al. (2007) who adopted $\log\epsilon(\text{Ba}) = 2.13$. The filled circles represent the turnoff stars, the open circles (in red in the electronic version of the paper) the RGB mixed giants and the open squares (in blue) the unmixed RGB giants. The two (“pink”) star-symbols represent the two carbon-rich stars we have measured (see Table 1). The thick (green) lines represent the mean slopes computed between $[\text{Fe}/\text{H}] = -3.6$ and $[\text{Fe}/\text{H}] = -2.6$. The slope of the regression line is slightly shallower when non-LTE effects are taken into account. In plot **b**) (NLTE) the thin (green) lines are drawn at a distance of two sigmas from the regression line. The two carbon-rich stars are outside the two sigmas limit. If we consider only the “normal” stars (not carbon rich) then 3 stars are outside this limit on the “Ba-rich” side.

Acknowledgements. The authors thank the referee for a very careful reading of the manuscript and for useful suggestions. S.M.A. kindly acknowledges the support and hospitality of the Paris-Meudon Observatory. P.B. acknowledges financial support from EU contract MEXT-CT-2004-014265(CIFIST). M.S., R.C., F.S., P.B., V.H., P.F. acknowledge the support of CNRS (PNG and PNPS).

References

- Allen, C. W. 1973, *Astrophysical Quantities* (London: Athlone Press)
- Andrievsky, S. M., Spite, M., Korotin, S. A., et al. 2007, *A&A*, 464, 1081
- Andrievsky, S. M., Spite, M., Korotin, S. A., et al. 2008, *A&A* 481, 481
- Asplund, M. 2005, *Ann. Rev. Astro. Astrophys.*, 43, 481
- Asplund, M., Grevesse, N., & Sauval, A. J. 2005, *ASP Conf. Ser.*, 336, 25
- Ballester, P., Modigliani, A., Boitquin, O., et al. 2000, *ESO Messenger*, 101, 31
- Barklem, P. S., Christlieb, N., Beers, T. C., et al. 2005, *A&A*, 439, 129
- Beers, T. C., & Christlieb, N. 2005, *ARA&A*, 43, 531
- Bonifacio, P., Molaro, P., Sivarani, T., et al. 2007, *A&A*, 462, 851 (First stars VII)
- Bonifacio, P., Spite, M., Cayrel, R., et al. 2009, *A&A*, submitted (First stars XII)
- Bruls, J. H., Rutten, R. J., & Shchukina, N. 1992, *A&A*, 265, 237
- Burris, D. L., Pilachowski, C. A., Armandro, T. A., et al. 2000, *ApJ*, 544, 302
- Carlsson, M. 1986, *Uppsala Obs. Rep.* 33

- Cameron, A. G. W. 1982, *Ap&SS*, 82, 123
- Cayrel, R., Hill, V., Beers, T. C., et al. 2001, *Nature*, 409, 691
- Cayrel, R., Depagne, E., Spite, M., et al. 2004, *A&A*, 416, 1117 (First Stars V)
- Crandall, D. H., Dunn, G. H., Gallagher, A., et al. 1974, *ApJ*, 191, 789
- Curry, J. J. 2004, *J. Phys. Chem. Ref. Data*, 33, 725
- Davidson, M. D., Snoek, L. C., Volten, H., & Doenszelmann, A. 1992, *A&A*, 255, 457
- Dekker, H., D'Odorico, S., Kaufer, A., et al. 2000, in *Optical and IR Telescopes Instrumentation and Detectors*, ed. I. Masanori, & A. F. Morwood, *Proc. SPIE*, 4008, 534
- Depagne, E., Hill, V., Spite, M., et al. 2002, *A&A*, 390, 187 (First Stars II)
- Drawin, H.-W. 1961, *ZPhy*, 164, 513
- Feeney, R. K., Hooper, J. W., & Elford, M. T. 1972, *PhRvA*, 6, 1469
- François, P. 1996, *A&A*, 313, 229
- François, P., Depagne, E., Hill, V., et al. 2007, *A&A*, 476, 935 (First stars VIII)
- Gigas, D. 1988, *A&A*, 192, 264
- Grevesse, N., & Sauval, A. J. 2000, *Origin of the elements in the Solar system*, ed. O. Manuel, 261
- Gustafsson, B., Edvardsson, B., Eriksson, K., et al. 2008, *A&A*, 486, 951
- Hill, V., Plez, B., Cayrel, R., et al. 2002, *A&A*, 387, 560 (First Stars I)
- Hofsaess, D. 1979, *ADNDT*, 24, 285
- Honda, S., Aoki, W., Kajino, T., et al. 2004, *ApJ*, 607, 474
- Korotin, S. A., Andrievsky, S. M., & Luck, R. E. 1999, *A&A*, 351, 168
- Kurucz, R. L. 1992, *The Stellar Population of Galaxies*, ed. B. Barbuy, & A. Renzini, *IAU Symp.*, 149, 225
- Kurucz, R. L. 1996, *Model Atmospheres and Spectrum Synthesis*, ed. S. J. Adelman, F. Kupka, & W. W. Weiss, San Francisco, *ASP Conf. Ser.*, 108, 2
- Kurucz, R. L., Furenlid, I., Brault, J., & Testerman, L. 1984, *Solar Flux Atlas from 296 to 1300 nm*, New Mexico, National Solar Observatory
- Lai, D. K., Bolte, M., Johnson, J. A., et al. 2008 [[arXiv:0804.1370v1](https://arxiv.org/abs/0804.1370v1)]
- Lang, K. 1998, *Astrophysical formulae* (Berlin – Heidelberg – New York: Springer-Verlag), 52
- Mashonkina, L., & Bikmaev, I. 1996, *ARep*, 40, 94
- Mashonkina, L., & Gehren, T. 2000, *A&A*, 364, 249
- Mashonkina, L., & Gehren, T. 2001, *A&A*, 376, 232
- Mashonkina, L., & Zhao, G. 2006, *A&A*, 456, 313
- Mashonkina, L., Gehren, T., & Bikmaev, I. 1999, *A&A*, 343, 519
- Mashonkina, L., Gehren, T., Travaglio, C., & Borkova, T. 2003, *A&A*, 397, 275
- Mashonkina, L., Zhao, G., Gehren, T., et al. 2008, *A&A*, 478, 529
- Miles, B. M., & Wise, W. L. 1969, *ADNDT*, 1, 1
- Peart, B., Underwood, J. R. A., & Dolder, K. 1989, *JPhB*, 22, 1679
- Peterson, R. C., Kurucz, R. L., & Carney, B. W. 1990, *ApJ*, 350, 173
- Rutten, R. J. 1978, *SoPh*, 56, 237
- Schoening, T., & Butler, K. 1998, *A&AS*, 128, 581
- Short, C. I., & Hauschildt, P. H. 2006, *ApJ*, 641, 494
- Snedden, C., McWilliam, A., Preston, G. W., et al. 1996, *ApJ*, 467, 819
- Sobelman, I. I., Vainshtein, L. A., & Yukov, E. 1981, *Excitation of Atoms and Broadening of Spectral Lines*, *Springer Ser. in Chem. Phys.* (Berlin: Springer)
- Spite, M., Cayrel, R., Plez, B., et al. 2005, *A&A*, 430, 655 (First Stars VI)
- Spite, M., Cayrel, R., Hill, V., et al. 2006, *A&A*, 455, 291 (First Stars IX)
- Steenbock, W., & Holweger, H. 1984, *A&A*, 130, 319
- Takeda, Y. 1991, *A&A*, 242, 455
- Travaglio, C., Gallino, R., Arnone, E., et al. 2004, *ApJ*, 601, 864
- Unsöld, A. 1968, *Physik der Sternatmosphären* (Berlin, Heidelberg, New York: Springer-Verlag), 332
- van Regemorter, H. 1962, *ApJ*, 136, 906
- Warner, B. 1968, *MNRAS*, 139, 115
- Wasserburg, G. J., & Qian, Y. Z. 2008 [[arXiv:0809.2827](https://arxiv.org/abs/0809.2827)]
- Wiese, W. L., & Martin, G. A. 1980, *NSRDS-NBS 68*, P.II